Supplementary Materials

HDAC10 Regulates Cancer Stem-like Cell Properties in KRAS-driven Lung Adenocarcinoma

Yixuan Li[1], Xiangyang Zhang[2], Shaoqi Zhu[3], Eden A. Dejene[1], Weiqun Peng[3], Antonia Sepulveda[4], Edward Seto[1]*

Table of Contents

Supplementary Materials and Methods

LUAD and Tumor sphere assay

To perform the rescue experiments, LUAD cells were transduced with lentiviral vectors expressing either wild-type HDAC10 or control vector (pLenti) and cultured with 0.5 mg/ml G418 for selection and maintenance of the stably expressing cells. To study the effect of SOX9 and SLUG on tumor sphere growth, LUAD cells were transduced with lentiviral vectors expressing either scrambled control shRNA (shNC) or shRNA targeting mouse SOX9 or SLUG. The transduced cells were cultured with 1 μg/ml Puromycin for selection.

The tumor sphere assay was performed under low-adherent, low-serum and low-cell density conditions, which have been previously described as stem cell-selective conditions. In brief, LUAD cells were suspended in 0.6% methylcellulose (Sigma-Aldrich)-based advanced DMEM/F12 medium (Gibco) supplemented with 20 ng/ml epidermal growth factor, B27 supplement and 2% FBS, and plated at 200 cells per well in ultra-low attachment 24-well plates (Corning, NY, USA). Cells were cultured for 1-2 weeks and the number of tumor spheres was counted under a light microscope with a 4× objective lens. The sphere formation efficiency was calculated by the following formula: sphere%= (No. of spheres counted/No. of cells seeded per well) ×100.

Plasmids and antibodies

Lentiviral pLenti-CMV-Neo-DEST/HDAC10 was constructed as described previously (1). The pLKO.1-sh-mSOX9-1 and pLKO.1-sh-mSOX9-2 plasmids were a gift from Bob Weinberg (Addgene plasmids 40645 and 40646). Lentiviral shRNA expression PLKO.1 plasmid targeting mouse SLUG was obtained from Sigma-Aldrich (TRCN0000096227). Lentiviral shRNA plasmid targeting human HDAC10 was obtained from Thermo Fisher Scientific (TRCN0000004861). Lentivirus was prepared by transfecting HEK 293T cells with the lentiviral plasmid together with packaging vectors. Lentivirus-transduced cells were selected for Neomycin (G418) or Puromycin resistance.

Rabbit anti-HDAC10 (H3413) antibody was purchased from Sigma-Aldrich. Polyclonal anti-SLUG/SNAI2 (9585), anti-p-SMAD2 (3101), anti-SMAD2 (5339), anti-p-ERK (9101), anti-ERK (9102), anti-RAS (G12D mutant specific) (14429) and anti-RAS (8955), anti-F4/80 (70076) antibodies were from Cell Signaling Technology (Danvers, MA). Rabbit anti-SOX9 (AB5535), anti-SFTPC (AB3786) and anti-SCGB1A1 (07-623) antibodies were from EMD Millipore. Rabbit anti-NOG (AF719) antibody was from Novus Biologicals. Anti-FOXJ1 (14-9965-80) and anti-Ki67 (14-5698) antibodies were from Ebioscience. Mouse anti-vinculin (sc-73614) antibody was from Santa Cruz Biotechnology. Anti-MAC-2 (CL8942AP) was from Cedarlane and anti-TTF-1 (07601MI) was from Thermo Fisher Scientific. The fluorochrome-labeled monoclonal antibodies against CD44 (103011), CD31 (102523), CD45 (103107), CD45 (103153), CD11b (101215) and EPCAM (118205) were from Biolegend. The fluorochrome-labeled monoclonal antibody against F4/80 (48-4801-80) was from eBioscience.

Xenograft mouse model

To quantify the tumor initiating capacity of LUAD cells, the limiting diluted cells were suspended in 1×PBS and mixed with equal volume of 50% Matrigel (in 1×PBS) before injection. LUAD cells (from 1×10^5 to 100) were subcutaneously transplanted into the left and right flank of athymic nude mice at the age of 6–8 weeks (Jackson Laboratory, Bar Harbor, ME, USA). Mice were evaluated every other day for tumor development. Three weeks after implantation, mice were sacrificed, and tumor weights determined.

Immunoblotting, histopathological and immunohistochemistry analyses, and EdU staining

Western blotting and immunostaining were performed as described previously (1). For immunostaining, cells cultured on coverslips were washed with PBS and fixed in either 4% paraformaldehyde for 15 min at room temperature. Fixed cells were permeabilized in PBS containing 0.5% Triton X-100 for 5 min and blocked in 3% bovine serum albumin in PBS for 30 min. Cells were then incubated with primary antibodies at 4°C overnight, followed by a 1-h incubation with secondary

antibody. Cells were washed, and nuclei were counterstained with DAPI (Invitrogen). Images were captured using fluorescence microscopy.

For histopathological analysis, mouse lungs were fixed by intratracheal instillation of 10% neutral buffered formalin and embedded in paraffin, and lung sections were stained with hematoxylin and eosin (H&E). Tumor burden was calculated as the sum of the total tumor area divided by the total lung area. The cell proliferation in tumors and macrophage recruitment was determined by immunohistochemical analysis using anti-Ki67 and anti-F4/80 antibodies. Sections were deparaffinized, antigens were retrieved and endogenous peroxidase was quenched for immunohistochemistry (IHC). After the primary antibodies and secondary antibodies incubation, the signal was detected with DAB peroxidase (HRP) substrate or slides were viewed using a light microscope. Staining intensity was scored by counting the number of positive cells in randomly selected fields. The immunofluorescent staining of SOX9 and Ki67 were performed using fluorescent conjugated secondary antibodies.

To measure cell proliferation in vivo, mice at 16 weeks of age were intraperitoneally injected with 200 μg of EdU and sacrificed 48 hours later. Mouse small intestines (positive control) and lungs were harvested. Tissues were formalin-fixed, embedded in paraffin, and sectioned. EdU staining was conducted using Click-iT™ EdU imaging kit (Invitrogen, Carlsbad, CA) according to the manufacturer's protocol. Cells were counterstained with Hoechst and imaged by fluorescence microscopy.

Flow cytometry

Flow cytometric analysis of the stem-like cancer cell population was performed using fluorochrome-labeled mAb (anti-CD44, CD31, CD45, EpCAM) and the LIVE/DEAD Fixable dye (L34963) from Thermo Fisher Scientific. The percentage of $EpCAM^{pos}$, $CD44^{pos}$, $CD45^{neg}$, $CD31^{neg}$ population was acquired on the BD Celesta Cell Analyzer. Expression of CD44 in LUAD cells was also evaluated by flow cytometry using APC rat anti-mouse CD44 antibody. Dead cells or cell debris were gated out using LIVE/DEAD dye. The analysis of the macrophage population was performed using

fluorochrome-labeled mAb against CD45, CD11b and F4/80. All the data were analyzed using FlowJo software.

RNA sequencing and pathway analysis

Total RNAs were isolated from *Hdac10* KO and WT tumor tissues by using the mirVana miRNA isolation kit (Applied Biosystems). The pure polyadenylated RNAs were isolated with the Dynabeads® mRNA Direct™ Micro Kit and sequencing libraries were constructed. Sequencing was carried out using the Ion Proton system. We sequenced *Hdac10* WT and KO tumor samples with approximately 19-25 million reads per sample. Raw data was aligned to the mouse reference genome. After filtering, the aligned reads were normalized and quantified using the DEseq2 algorithm by the StrandNGS program. Statistical analysis was performed using the Moderated T-Test to determine significant differentially expressed genes (DEGs) that were upregulated by at least 1-fold with various p-values. We were able to detect 1189 genes that were significantly differentially regulated between KO and WT out of 38,087. The cutoffs are p values <0.05 and fold change ≥ 2.0.

Real-time RT-PCR

Total RNA was isolated from cells with the mirVana miRNA isolation kit (Applied Biosystems) and reverse transcription was carried out using the qScript cDNA synthesis kit (Quanta Biosciences). Relative quantitation of mRNAs was carried out via SYBR green-based quantitative PCR using a Quantstudio 3 Real-time PCR system (Applied Biosystems). PCR results were analyzed using the $2^{-(\Delta\Delta CT)}$ method.

Reference

1. Li Y., Peng L. and Seto E. Histone Deacetylase 10 Regulates the Cell Cycle G2/M Phase Transition via a Novel Let-7-HMGA2-Cyclin A2 Pathway. Mol Cell Biol 2015;35:3547-65

Table S1. Primer sequences for real-time RT-PCR

Primer Name	Sequence
mHDAC10-exon1-S	TAGTTAGGTGAGACCGGGCA
mHDAC10-exon1-AS	TCCTCGTGGTACACAAGTGC
mHDAC10-exon7/8-S	CTGATGCAGATGCAGTTGGC
mHDAC10-exon7/8-AS	CACCAGCACCAACTCAGGAT
mHDAC10-exon10/12-S	TTTGTGCTGTGTTGGAGGGT
mHDAC10-exon10/12-AS	TTTTGCTGGAGGCTTGTCCA
mALDH1A1-S	AGGGGACAAGGCTGATGTTG
mALDH1A1-AS	TGCAGCCTCCTAAATCCGAC
mCD133-S	TCAGTGCCCTGCTGTTACTG
mCD133-AS	AGAGGGCAATCTCCTTGGAA
mOCT4-S	GGAGGGATGGCATACTGTGG
mOCT4-AS	TTTCATGTCCTGGGACTCCTC
mNANOG-S	GAGCCGTTGGCCTTCAGATA
mNANOG-AS	ATGGCGAGGGAAGGGATTTC
mSOX2-S	CAAAAACCGTGATGCCGACT
mSOX2-AS	CGCCCTCAGGTTTTCTCTGT
mSOX9-S	CGTGCAGCACAAGAAAGACC
mSOX9-AS	AGATTGCCCAGAGTGCTCG
INHBA-S	GTGCTGCTCAAGTGCCAATAC
INHBA-AS	GTTTTGTCAGCCGGCTCTTG
mNODAL-S	TCTCAGGTCACGTTTGCCTC
mNODAL-AS	TTTCTGCTCGACTGGACACC
mNOG-S	CCTGGTGGACCTCATCGAAC
mNOG-AS	GGGGGCGAAGTAGCCATAAA
mSERPINE1-S	AGCTTTGTGAAGGAGGACCG
mSERPINE1-AS	AAGGTGCCTTGTGATTGGCT
mSLUG-S	CTCACCTCGGGAGCATACAG
mSLUG-AS	GACTTACACGCCCCAAGGATG
mCCNA2-S	CTCGCTGCATCAGGAAGACC
mCCNA2-AS	TAAGAGGAGCAACCCGTCG
mCCND2-S	GACAACTCTGTGAAGCCCCA

mCCND2-AS	AACTTGAAGTCGGTAGCGCA
mCDC25C-S	TCATGGCCACAGAAAGAAGATT
mCDC25C-AS	TCATTTCCAGCTCACACAGAGG
mFOXM1-S	GGCCTTCCACAGATGCTCTC
mFOXM1-AS	GGAACTGGACTCTGTTGGCA
mSMAD3-S	AAGAAGCTCAAGAAGACGGGG
mSMAD3-AS	CAGTGACCTGGGGATGGTAAT
mSMAD7-S	TTTTCTCAAACCAACTGCAGGC
mSMAD7-AS	CCCAGGGGCCAGATAATTCG
mNCOR2-S	TCTGGAGACCTGGTACGGAG
mNCOR2-AS	GACAGGCGAAGAGGTGGAG
mSCGB1A1/CC10-S	CATCATGAAGCTCACGGAGA
mSCGB1A1/CC10-AS	AGGGCAGTGACAAGGCTTTA
mAGR3-S	CTTCGCAACGCGTAACATCC
mAGR3-AS	CCCCATCCTCTTGAGAGTGTCT
mKRT5-S	GCAGACACACGTCTCTGACA
mKRT5-AS	GGTTGGCACACTGCTTCTTG
mKRT14-S	CTACCTGGACAAGGTGCGTG
mKRT14-AS	TGCTCCGTCTCAAACTTGGT
mSFTPC-S	TTCCGAGTCCGATTCTTCCG
mSFTPC-AS	CGGTTTCTACCGACCCTGTG
mFOXJ1-S	CTCTGAGCCAGGCCTCACATT
mFOXJ1-AS	GGTCAACATCCACAGGCTGA
mWNT3-S	GTCCAAGCTGCCTCTACTCG
mWNT3-AS	AAATGGGAGTCGACGGACAA
mWNT7A-S	CGGACGCCATCATCGTCATA
mWNT7A-AS	CAGTTCCAACGGCCATTTCG
mWNT7B-S	ATCGACTTTTCTCGTCGCTTT
mWNT7B-AS	CGTGACACTTACATTCCAGCTTC
mWNT10A-S	TCAGACAGCTGGGGGTGATA
mWNT10A-AS	TTGCCTATCACTCCTGGGGA
mWNT10B-S	CCGTGAGTTAGGTCGAGCAG
mWNT10B-AS	CGGGAGGAAGGGAGGGTAAA

Table S2. The incidence of the accumulation of alveolar macrophages

Genotype	Mice age (weeks)	Total mice No.	Mice No. with lung macrophage infiltration	Incidence[#]
HDAC10$^{+/+}$ *Kras*^{LA1}	8-9	8	0	0%
	16-19	7	1	14%
	30-33	5	1	20%
HDAC10$^{-/-}$ *Kras*^{LA1}	8-9	11	1	9%
	16-19	7	2	28.60%
	30-33	6	5	83%

[#] Incidence = (mice No. with lung macrophage infiltration / total mice No.)×100%.

Figure S1

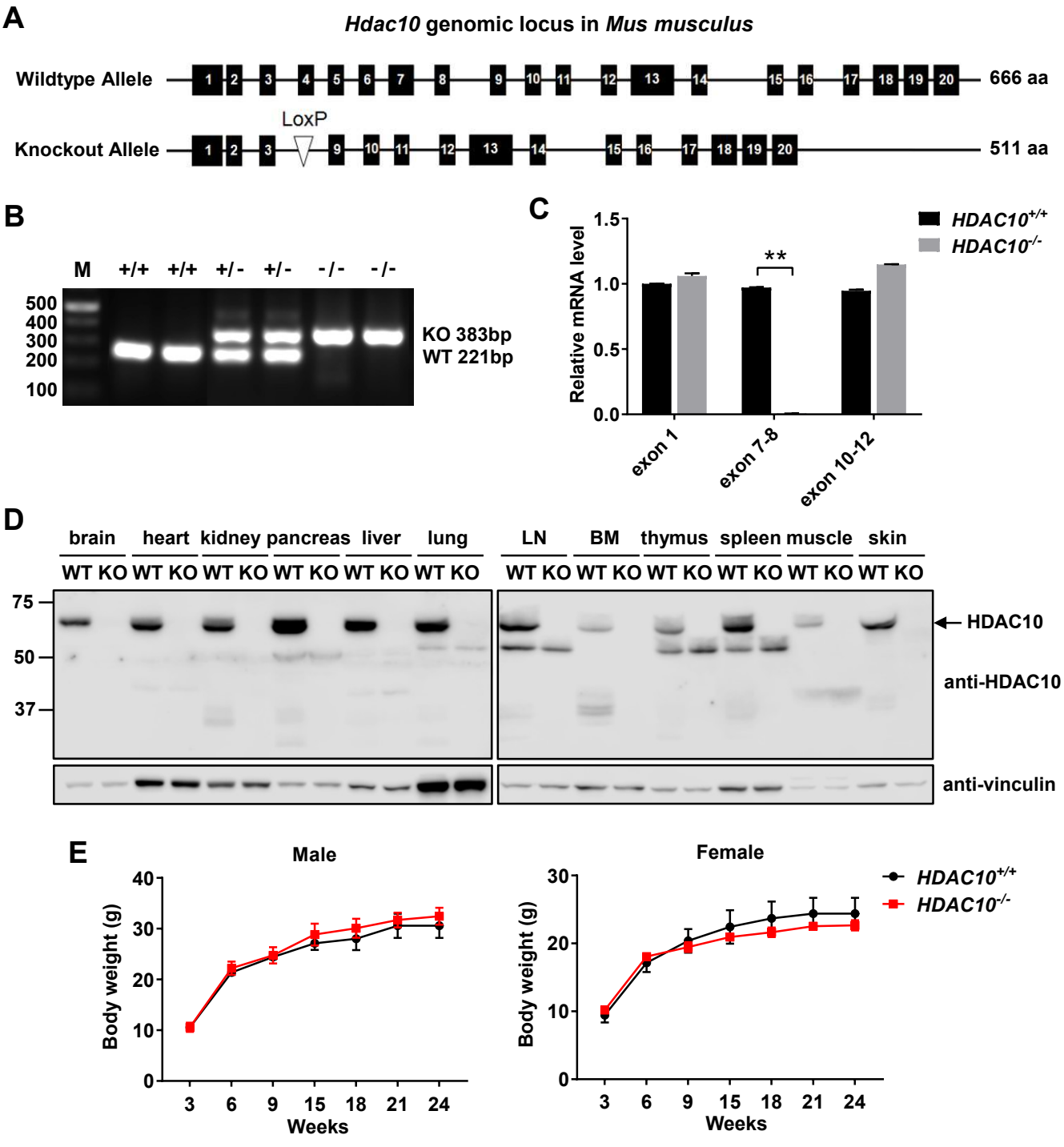
A
Hdac10 genomic locus in Mus musculus
Wildtype Allele
1 2 3 4 5 6 7 8 9 10 11 12 13 14 15 16 17 18 19 20
666 aa
LoxP
Knockout Allele
1 2 3 9 10 11 12 13 14 15 16 17 18 19 20
511 aa
B
M +/+ +/+ +/- +/- -/- -/-
500
400
300
200
100
KO 383bp
WT 221bp
C
HDAC10+/+
HDAC10-/-
Relative mRNA level
1.5
1.0
0.5
0.0
**
exon 1
exon 7-8
exon 10-12
D
brain heart kidney pancreas liver lung
LN BM thymus spleen muscle skin
WT KO WT KO WT KO WT KO WT KO WT KO
WT KO WT KO WT KO WT KO WT KO WT KO
75
50
37
HDAC10
anti-HDAC10
anti-vinculin
E
Male
Female
Body weight (g)
40
30
20
10
0
3 6 9 15 18 21 24
Weeks
HDAC10+/+
HDAC10-/-

Figure S2

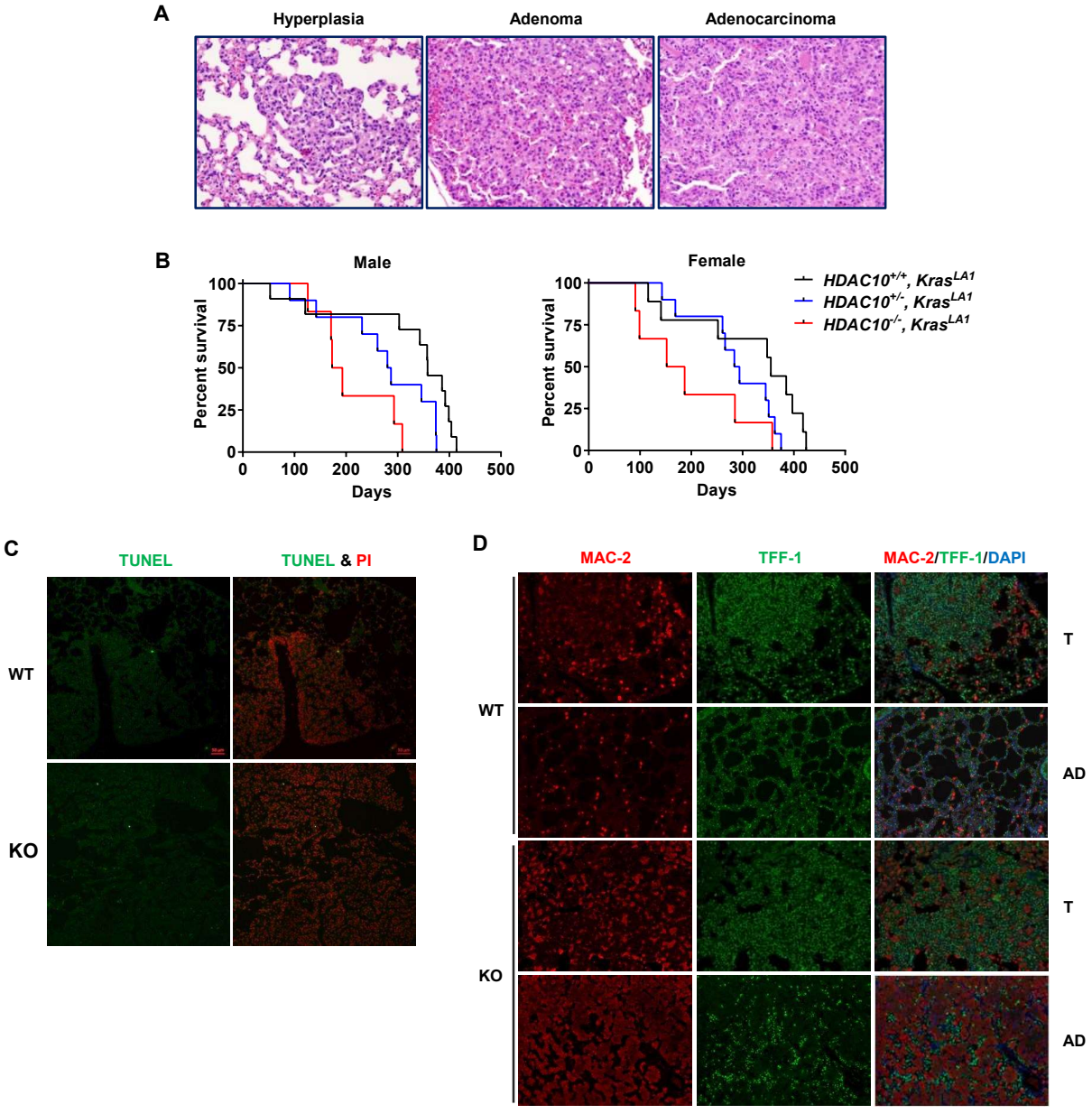
A
Hyperplasia
Adenoma
Adenocarcinoma
B
Male
Female
Percent survival
Days
HDAC10+/+, KrasLA1
HDAC10+/-, KrasLA1
HDAC10-/-, KrasLA1
C
TUNEL
TUNEL & PI
WT
KO
D
MAC-2
TFF-1
MAC-2/TFF-1/DAPI
WT
KO
T
AD
T
AD

Figure S3

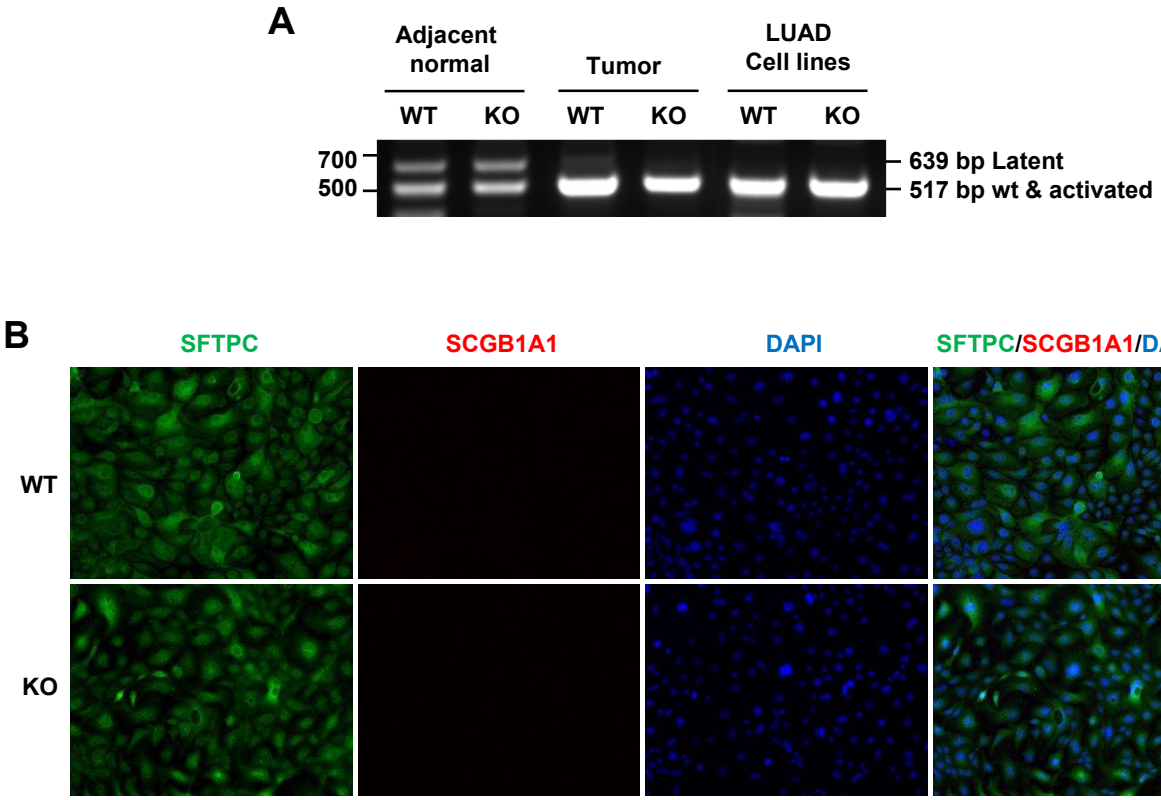
A
Adjacent normal
Tumor
LUAD Cell lines
WT
KO
WT
KO
WT
KO
700
500
639 bp Latent
517 bp wt & activated
B
SFTPC
SCGB1A1
DAPI
SFTPC/SCGB1A1/DAPI
WT
KO

Figure S4

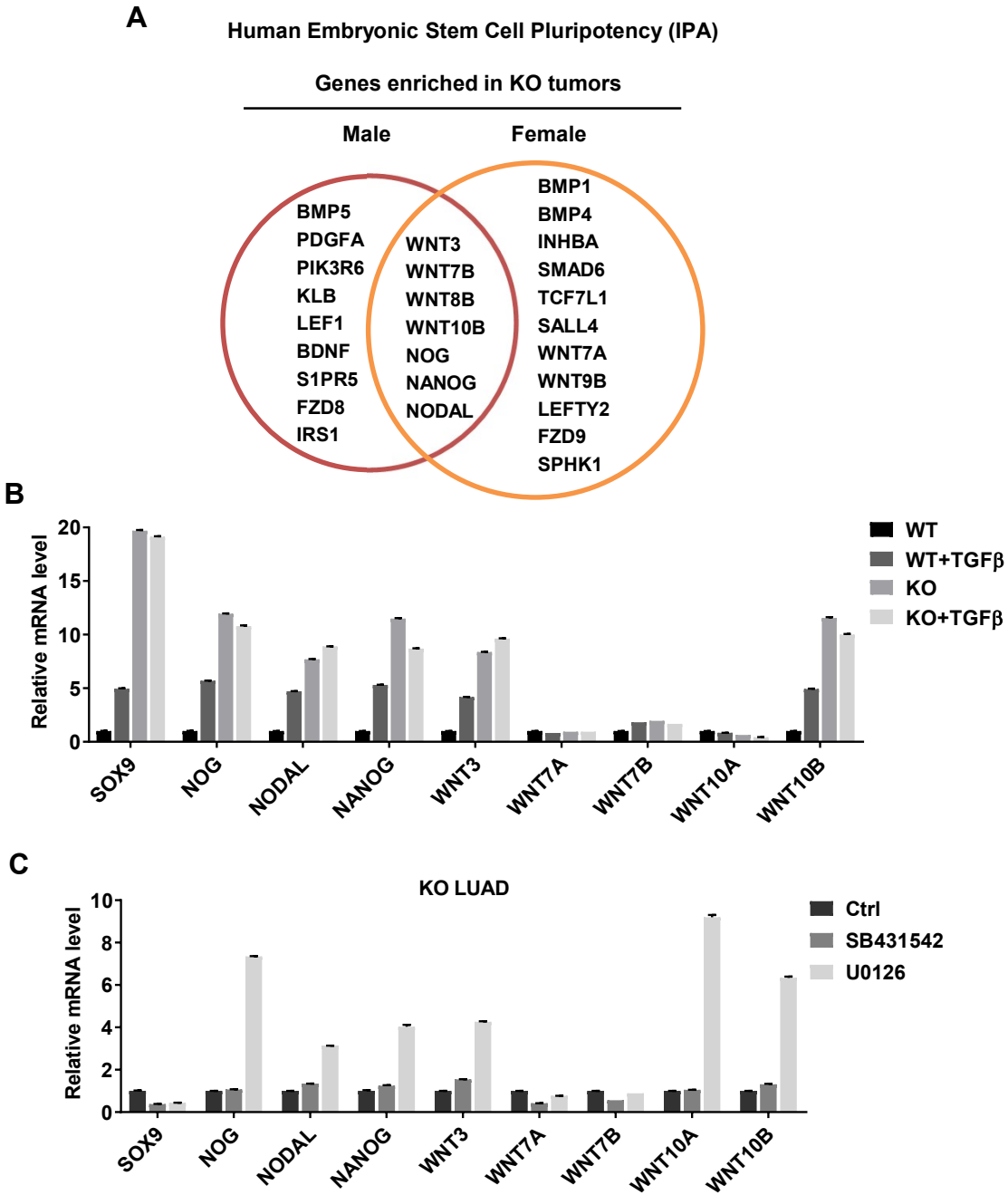
A
Human Embryonic Stem Cell Pluripotency (IPA)
Genes enriched in KO tumors
Male
Female
BMP5
PDGFA
PIK3R6
KLB
LEF1
BDNF
S1PR5
FZD8
IRS1
WNT3
WNT7B
WNT8B
WNT10B
NOG
NANOG
NODAL
BMP1
BMP4
INHBA
SMAD6
TCF7L1
SALL4
WNT7A
WNT9B
LEFTY2
FZD9
SPHK1
B
Relative mRNA level
20
15
10
5
0
WT
WT+TGFβ
KO
KO+TGFβ
SOX9
NOG
NODAL
NANOG
WNT3
WNT7A
WNT7B
WNT10A
WNT10B
C
KO LUAD
Relative mRNA level
10
8
6
4
2
0
Ctrl
SB431542
U0126
SOX9
NOG
NODAL
NANOG
WNT3
WNT7A
WNT7B
WNT10A
WNT10B

Figure S5

A

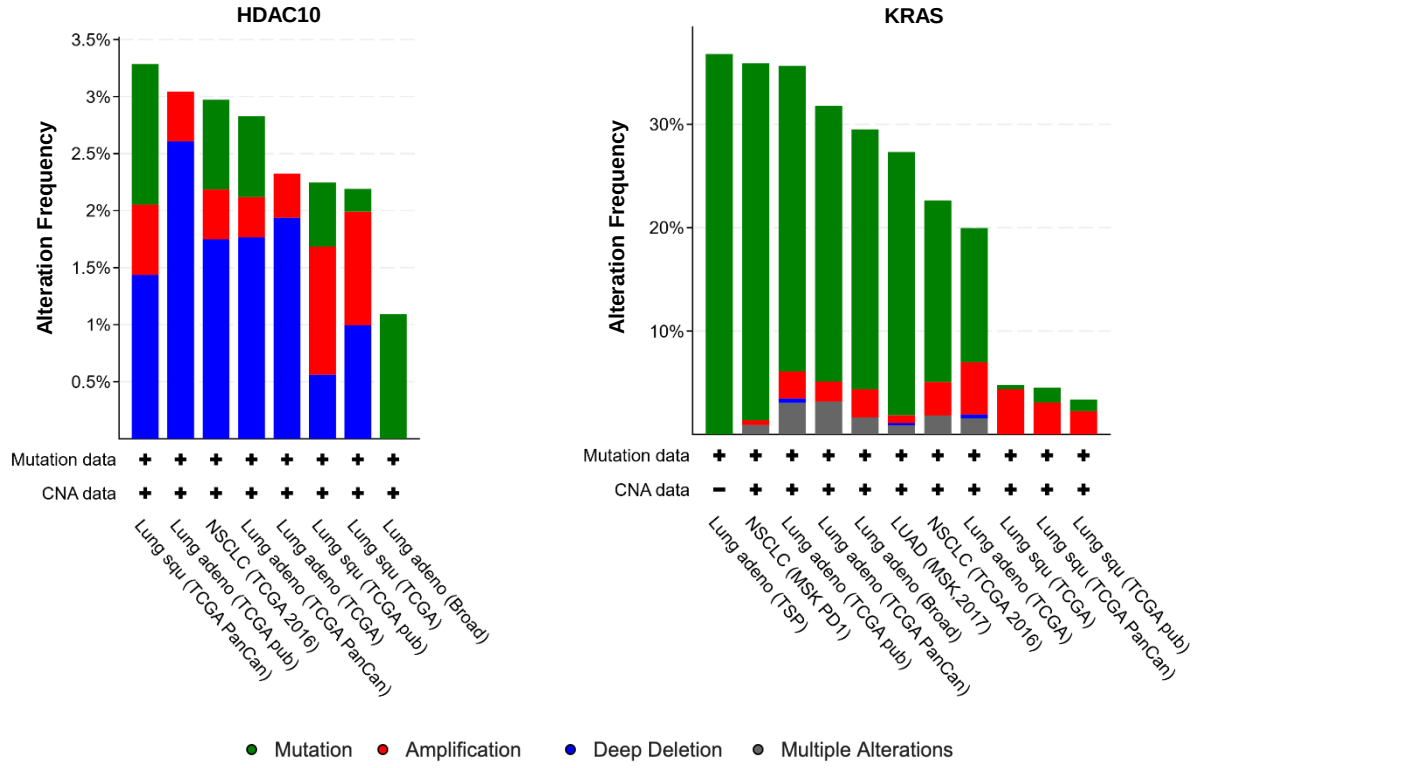
HDAC10
KRAS
Alteration Frequency
3.5%
3%
2.5%
2%
1.5%
1%
0.5%
30%
20%
10%
Mutation data
CNA data
Lung squ (TCGA PanCan)
Lung adeno (TCGA pub)
NSCLC (TCGA 2016)
Lung adeno (TCGA)
Lung adeno (TCGA PanCan)
Lung squ (TCGA)
Lung squ (TCGA pub)
Lung adeno (Broad)
Lung adeno (TSP)
NSCLC (MSK PD1)
LUAD (MSK 2017)
Mutation
Amplification
Deep Deletion
Multiple Alterations

B

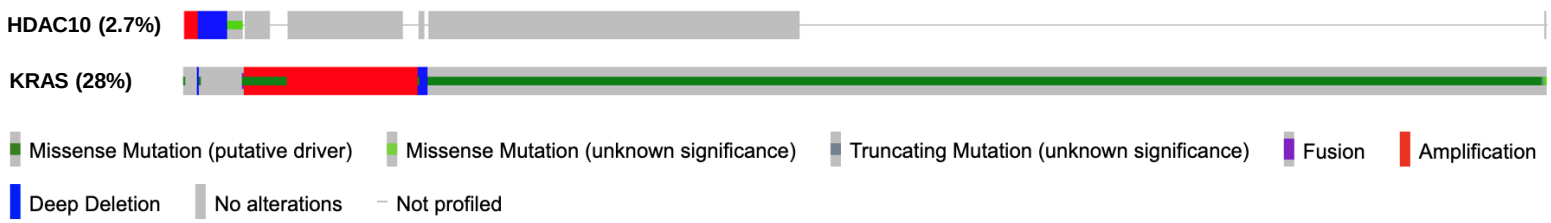
HDAC10 (2.7%)
KRAS (28%)
Missense Mutation (putative driver)
Missense Mutation (unknown significance)
Truncating Mutation (unknown significance)
Fusion
Amplification
Deep Deletion
No alterations
Not profiled

Supplementary Figure Legends

Figure S1. Generation of *Hdac10* KO mice by the Cre-loxP method. (A) Schematic representation of the *Hdac10* genomic locus in *Mus musculus* and the strategy to generate *Hdac10* KO mice by deleting the HDAC10 catalytic domain. (B) Genotyping was performed by PCR on genomic DNA isolated from the tail biopsies. (C) Real-time RT-PCR analysis of *Hdac10* mRNA levels using primers targeting HDAC10 exon 1, exons 7-8 and exons 10-12, respectively. (D) Western blot analysis of HDAC10 protein levels in indicated mouse tissues. (E) Body weights of *Hdac10* WT and KO mice (n=5) monitored twice a week.

Figure S2. Histopathological, immunohistochemistry and TUNEL analysis of lung tumors. (A) Representative hematoxylin and eosin staining of the lungs tumor with indicated benign and preinvasive lesions. (B) The Kaplan–Meier survival of mice with indicated genotypes and gender. (C) Representative TUNEL staining of *Hdac10* WT and KO tumors. (D) Immunofluorescent images of MAC-2 (macrophage marker) and TTF1 (lung epithelial marker) in tumor (T) and tumor adjacent (AD) tissues from mice at the age of 16 weeks. Nuclei were counterstained with DAPI.

Figure S3. Isolation and validation of primary mouse lung adenocarcinoma cells. (A) The RT-PCR result of the recombination of latent $Kras^{LA1}$ alleles in tumor and adjacent normal tissues, as well as cultured primary lung cancer cells. The latent 639 bp and wildtype or activated 517 bp PCR bands are indicated. (B) Immunofluorescent images of SFTPC (green), SCGB1A1 (red) and DAPI (blue) in LUAD cells.

Figure S4. Ingenuity Pathway Analysis of genes associated with embryonic stem cell pluripotency. (A) Venn diagram represents differentially expressed genes which relate to human ES cell pluripotency revealed by IPA. (B) Results of real-time RT-PCR analysis of the expression of pluripotency transcription

factors in *Hdac10* WT and KO LUAD cells treated with 5 ng/ml TGF-β or solvent control for 3 days. (C) Results of real-time RT-PCR analysis of the expression of pluripotency transcription factors in *Hdac10* WT and KO LUAD treated with 10 μM SB431542 (ALK5i) or 10 μM U0126 (MEKi) or solvent control for 3 days.

Figure S5. Genetic alterations of *HDAC10* in human lung cancer. (A) Genetic alterations of *HDAC10* and *KRAS* in different human lung cancer cohort studies form cBio Portal. (B) OncoPrint of genetic landscape of *HDAC10* and *KRAS* in TCGA lung adenocarcinoma cohorts.